TRANSIENT RESPONSE OF THE SOLAR WIND TO CHANGES IN FLOW GEOMETRY

Flows in Coronal Holes

S. S. HASAN and P. VENKATAKRISHNAN

Indian Institute of Astrophysics, Bangalore-560034, India

(Received 10 August; in revised form 11 December, 1981)

Abstract. The transient response of the solar wind to changes in geometry is examined. An initial stationary flow in a configuration that diverges as r^2 is assumed. This state corresponds to the usual solar wind solution. The effect on the flow through a tube whose area $A(r, t)$ diverges faster than r^2, with the degree of divergence increasing in time, is considered. The asymptotic form of $A(r, t)$ is chosen to mimic the form inferred in coronal holes. A detailed parameter study relating the form of $A(r, t)$ to the pattern of flow in the tube is presented. It is observed that in the limit of large time (large compared to τ, the time constant for change in geometry of a flow tube) the solutions obtained from a time-dependent analysis can depend upon τ. For sufficiently large τ, the asymptotic solution is the same as the steady state solution obeying the correct boundary conditions and possessing a smooth sonic transition. However, if the geometry changes rapidly enough, solutions exhibiting shock-like discontinuities can also exist. This is essentially a new feature that emerges from the present investigation. Finally, it is suggested that this study may be useful in describing flows in evolving coronal holes.

1. Introduction

The last two decades or so have witnessed numerous theoretical investigations of the solar wind (e.g. Parker, 1958, 1960, 1963, 1965). It is now generally recognized that the solar wind is a consequence of the expansion of coronal material into interplanetary space (Parker, 1958). A number of detailed theoretical studies exist which have examined this expansion assuming spherically symmetric flow (see Hundhausen, 1972, and references therein). Recent observations of coronal holes have focussed interest on generalizing previous studies to nonspherically symmetric flow (e.g. Kopp and Holzer, 1976, henceforth referred to as KH; Steinolfson and Tandberg-Hanssen, 1977; for reviews see Holzer, 1976; Suess, 1979).

Coronal holes are regions of open magnetic field lines (Altschuler *et al.*, 1972) characterized by a reduced density compared to their surroundings (Munro and Withbroe, 1972). Furthermore, coronal holes are believed to be the sources of certain high speed streams observed in the solar wind (Krieger *et al.*, 1973). It is also believed that the area of a flow tube in a coronal hole region diverges faster than r^2, where r is the heliocentric distance (Munro and Jackson, 1977). Further details on coronal holes can be found in Zirker (1977).

For steady isothermal expansion in a radial geometry, the existence of a continuous transonic solution that extends from the corona to the interplanetary medium was discussed by Parker (1958) (see also Parker, 1960). It was shown that the transition from

Solar Physics **80** (1982) 385–403. 0038–0938/82/0802–0385$02.85.

subsonic to supersonic flow occurred through a critical point of the fluid equations. A generalization to the case when the geometry was nonradial revealed the existence of multiple critical points (Parker, 1963). A detailed examination of solar wind flow in coronal holes by KH showed that a continuous solution was still posible in the presence of multiple critical points. For sufficiently rapid nonradial divergence they found that the sonic transition occurs much closer to the Sun than for the radial case. However, as noted by these authors, use of the steady equations did not permit them to study the transient readjustment of the flow from a geometry which supports a slow expansion to one in which fast expansion occurs. Such a study is of considerable interest especially when the final steady topology has multiple critical points. When examining the transient response, it is not clear a priori through which critical point the sonic transition occurs. In this paper, we address ourselves to such questions using a time-dependent approach. Furthermore, such an investigation is useful for describing the flow in coronal holes during their initial development which according to observations, takes place on a time scale of the order of hours (Solodyna *et al.*, 1977).

Let us briefly summarize the plan of study that we undertake in this paper. Starting from an initial state with a radial geometry and for which there exists a steady continuous Parker solution, the temporal response of this flow to changes in flow geometry are investigated. By choosing a form for $A(r, t)$, the area of a flow tube, which simulates the form in coronal holes, a detailed parameter study relating the form of $A(r, t)$ to the flow pattern in the tube is presented. The conditions under which a transition from an initial steady radial configuration to a continuous final steady state with a faster than r^2 divergence take place are discussed. Finally, the relevance of this study to flows in coronal holes is pointed out.

2. Basic Equations

Let us consider a region in the corona where the magnetic field geometry is open and where plasma flows along the field lines. We assume that the flow is one-dimensional and radial, but that the cross-sectional area of a flux tube need not vary as r^2.

In a heliocentered co-ordinate system, the one fluid equations for one dimensional radial flow in a tube, assuming a polytropic equation of state and zero viscosity are:

$$\frac{\partial}{\partial t}(\rho A) + \frac{\partial}{\partial r}(\rho v A) = 0\,, \tag{2.1}$$

$$\rho\left(\frac{\partial v}{\partial t} + v\,\frac{\partial v}{\partial r}\right) = \frac{-\rho G M_\odot}{r^2} - \frac{\partial p}{\partial r}\,, \tag{2.2}$$

$$\left(\frac{\partial}{\partial t} + v\,\frac{\partial}{\partial r}\right) p/\rho^\alpha = 0\,, \tag{2.3}$$

where ρ, v, and p denote mass density, radial velocity, and pressure of the fluid respec-

tively, α is the polytropic index, r is the radial distance, G is the gravitational constant, and $M_\odot$ is the solar mass.

In Equations (2.1)–(2.3), we assume that $A(r, t)$ is known, leaving ρ, v, and p as the unknown flow variables which depend only on r and t. Transverse gradients are effectively incorporated by specifying the tube geometry at each space-time point in the same spirit as Kopp and Pneuman (1976) and Hasan and Venkatakrishnan (1981). Noting that Equations (2.1)–(2.3) are hyperbolic, we solve them by the method of characteristics (Courant and Friedrichs, 1948). The transformed equations are:

$$\frac{\mathrm{d}p_\pm}{\mathrm{d}t} \pm \rho a \frac{\mathrm{d}u_\pm}{\mathrm{d}t} = -\rho a^2 \left(u \frac{\partial \ln A}{\partial r} + \frac{\partial \ln A}{\partial t} \right) \mp a\rho \frac{GM_\odot}{r^2} \quad \text{along} \quad C_\pm , \tag{2.4a, b}$$

$$\frac{\mathrm{d}p_0}{\mathrm{d}t} - a^2 \frac{\mathrm{d}\rho_0}{\mathrm{d}t} = 0 \quad \text{along} \quad C_0 , \tag{2.5}$$

where $a = \sqrt{\alpha p/\rho}$ is the sound speed and $C_\pm$ and C_0 denote the characteristic curves, whose equations are:

$$C_\pm : \quad \left(\frac{\mathrm{d}r}{\mathrm{d}t} \right)_\pm = u \pm a , \tag{2.6a, b}$$

$$C_0 : \quad \left(\frac{\mathrm{d}r}{\mathrm{d}t} \right)_0 = u . \tag{2.7}$$

Equations (2.4a, b) and (2.5) are also referred to as the compatibility equations valid on the characteristics $C_\pm$ and C_0, respectively. Before solving these equations, it is necessary to specify the tube geometry through the function $A(r, t)$.

3. Tube Geometry

We chose a function $A(r, t)$ based on the requirement that initially the tube geometry is radial and asymptotically (in time) it approaches a stationary form, which has a faster than r^2 divergence. In order to keep the analysis sufficiently general we shall consider the following forms for $A(r, t)$ which satisfy the preceding requirement:

(a) $$A(r, t) = 2\pi r^2 \left[1 - \tfrac{1}{2} \cos \theta(r, t) \right] , \tag{3.1}$$

where

$$\theta(r, t) = \theta_i + \frac{\Delta\theta}{2} (1 - e^{-t/\tau}) \left[1 - \cos \left(\pi \frac{r - R_\odot}{R_m - R_\odot} \right) \right] , \quad R_\odot \le r \le R_m ,$$

$$\theta(r, t) = \theta_i + \Delta\theta (1 - e^{-t/\tau}) , \qquad r > R_m , \tag{3.2}$$

where θ_i, $\Delta\theta$, R_m, $R_\odot$ (the solar radius) and τ are constants. At a certain instant of time, the nonradial divergence occurs between $r = R_\odot$ to $r = R_m$ and the angular extent of the tube varies from θ_i at $R_\odot$ to $\theta_i + \Delta\theta(1 - e^{-t/\tau})$ beyond R_m. The symbol τ is the time constant for the nonradial expansion of the tube. This form for $A(r, t)$ in the limit $t \to \infty$ is the same as that considered by Steinolfson and Tandberg-Hanssen (1977).

(b)
$$\frac{A(r, t)}{A_\odot} = \left(\frac{r}{R_\odot}\right)^2 f(r, t)\,, \tag{3.3}$$

where

$$f(r, t) = \frac{f_{\max}(t)\, e^{(r - R_1)/\sigma} + f_1}{e^{(r - R_1)/\sigma} + 1}\,, \tag{3.4}$$

$$f_1 = 1 - (f_{\max}(t) - 1)\, e^{(R_\odot - R_1)/\sigma}\,, \tag{3.5}$$

and

$$f_{\max}(t) = F_i + F_m(1 - e^{-t/\tau})\,. \tag{3.6}$$

This form is essentially the one given by KH, with the difference that $f_{\max}$ in our case is a time-dependent function. The major nonradial divergence at some instant of time occurs for $R_1 - \sigma \le r \le R_1 + \sigma$, achieving a maximum at $r = R_1$. The function $f_{\max}$ varies from F_i at $t = 0$ to $F_i + F_m$ at $t = \infty$. Figure 1 depicts the boundary streamlines, as calculated from Equation (3.3) at different instants of time for $R_1 = 1.5R_\odot$, $\sigma = 0.1R_\odot$, $F_i = 1$, and $F_m = 11$.

4. Initial State

Since the problem under consideration is an initial value one, a knowledge of the state at $t = 0$ is necessary. Assuming an initial state that is independent of time, the flow variables can be easily determined by solving Equations (2.1)–(2.3) in the absence of the $\partial/\partial t$ terms. We consider two distinct cases for which the polytropic index α has the values 1.0 (isothermal state) and 1.1. In terms of the Mach number M and sound speed a related by

$$M^2 = v^2/a^2 = v^2\rho/\alpha p \tag{4.1}$$

the solution of the steady equations yields the following transcendental relationship between M^2 and r (Parker, 1958):

$$M^2 - \ln M^2 - \ln A^2 - 4/r = M_0^2 - \ln M_0^2 - \ln A_0^2 - 4/r_0\,, \tag{4.2}$$

where the subscript '0' denotes the values at some reference level. For $\alpha = 1.1$, the

relationship is (KH)

$$M^{4/(\alpha+1)} + \frac{2}{\alpha-1} M^{-2[(\alpha-1)/(\alpha+1)]} = \\ = \frac{g(r)}{g_0}\left[M_0^{4/(\alpha+1)} + \frac{2}{\alpha-1} M_0^{-2[(\alpha-1)/(\alpha+1)]}\right], \tag{4.3}$$

where

$$g(r) = A(r)^{2[(\alpha-1)/(\alpha+1)]}\left(E + \frac{GM_\odot}{r}\right) \tag{4.4}$$

and

$$E = \tfrac{1}{2}v^2 + \frac{\alpha}{\alpha-1} p/\rho - \frac{GM_\odot}{r}. \tag{4.5}$$

Equation (4.5) just expresses the fact that the total energy per gram E is a constant of the motion. For an initial geometry where $A(r) \sim r^2$, the solution topology exhibits a

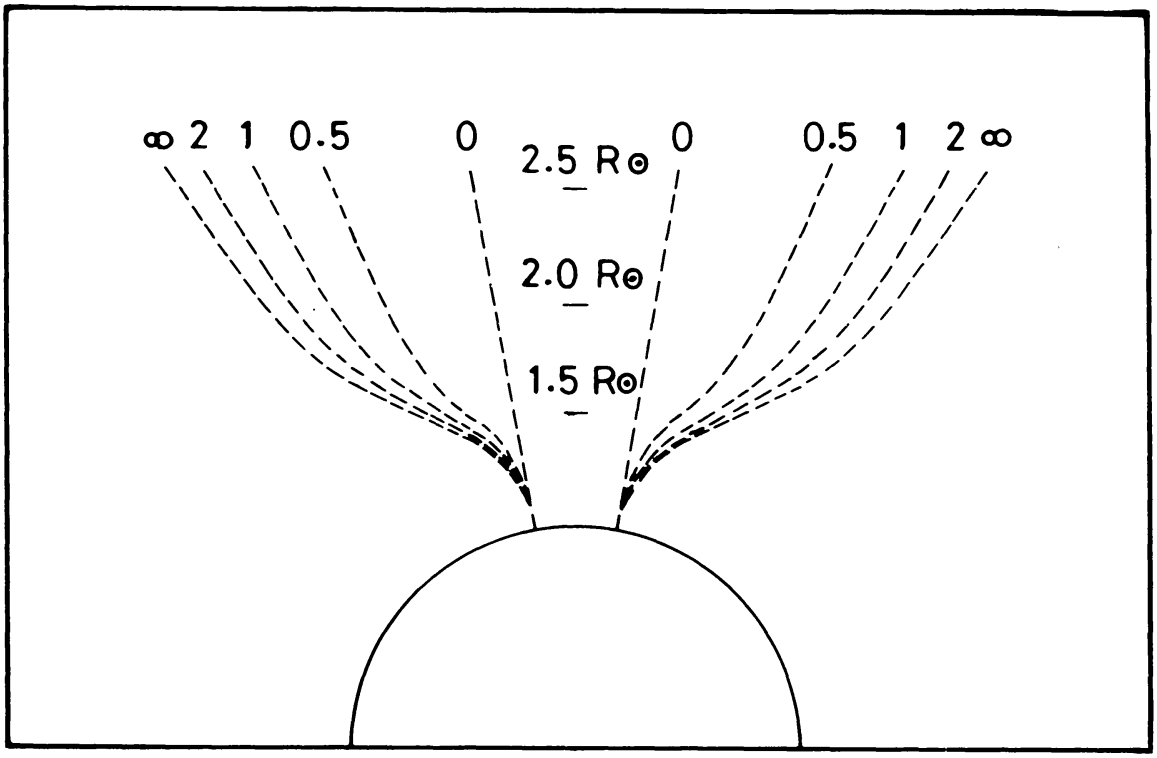

Fig. 1. The boundary streamlines of a coronal hole at different epochs (t/τ) of its temporal evolution are shown assuming $F_i = 1$, $F_m = 11$, $R_1 = 1.5R_\odot$ and $\sigma = 0.1R_\odot$. An angular width of 20° is assumed at the base.

critical point at which $M = 1$ when $r = r_c$, where

$$r_c = \begin{cases} \dfrac{GM_\odot}{2a^2} & \text{for} \quad \alpha = 1\,, \qquad (4.6a) \\ \dfrac{GM_\odot}{E}\,\dfrac{5-3\alpha}{4(\alpha-1)} & \text{for} \quad \alpha \neq 1\,. \qquad (2.6b) \end{cases}$$

It is worth mentioning here that for $A(r)$ increasing faster than r^2, multiple critical points can arise, which mathematically correspond to turning points of the differential equation for M (for details on the origin and nature of critical points in the solar wind (see Holzer, 1977).

5. Method of Solution

Once the initial state of the fluid is known, the time-dependent set of Equations (2.4a, b), (2.5), (2.6a, b), and (2.7) can be used to determine the state of the fluid at a subsequent instant of time. For solving these equations, a two-dimensional grid consisting of the C_+, C_-, and C_0 characteristics is prepared. When solving time-dependent flow problems a certain amount of care must be exercised in the choice of boundary conditions in order to avoid spurious effects. At the base of the tube where the flow is subsonic, only the C_- characteristic reaches points on the boundary from within the tube. Consequently, only two flow variables can be specified there while the third has to be determined from the compatibility relation (2.4b). If the flow is supersonic at the outer boundary, then no boundary conditions should be specified, as all three characteristics originate within the tube and the flow variables can be calculated from the compatibility relations. For simplicity, we assume that at the base of the tube the pressure and density are constant. The outer boundary for the isothermal case is taken at $r = 3R_\odot$ where the flow is supersonic. In the study of the polytropic case, choosing an outer boundary beyond $r = 4.5R_\odot$, which is where the normal solar wind becomes supersonic, is uneconomic in terms of computer time. Hence for practical considerations, we choose the outer boundary at $r = 2.6R_\odot$. In this case we impose one boundary condition, viz. the boundary velocity is the extrapolated value from two preceding space points.

Equations (2.4)–(2.7) were solved numerically using a predictor-corrector method. An inverse matching scheme was used to advance the equations in time (for details see Hasan and Venkatakrishnan, 1980). To ensure numerical stability, the time step was chosen small enough to satisfy the Courant Friedrichs Lewy criterion.

The optimum spatial grid size was chosen by keeping the area fixed at its initial value and studying the flow such that within 100 time steps the velocity at any space point varied by less than 5%. For the isothermal case, 40 grid points corresponding to a step length of $0.050R_\odot$ were found adequate. However, for the polytropic case where the base

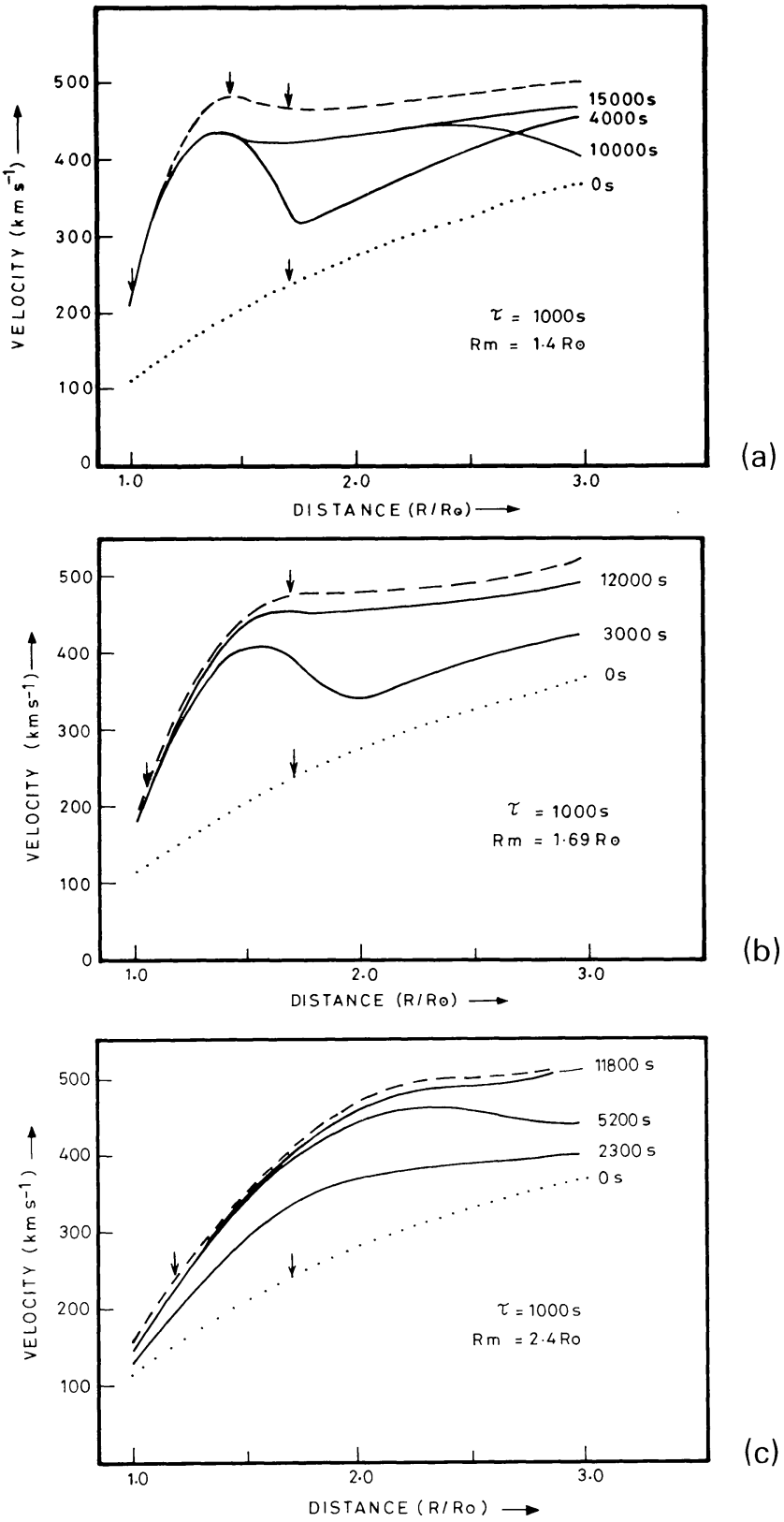

Fig. 2. The radial variation of velocity at different instants of time is shown in the isothermal case assuming $\tau = 1000$ s and $T = 3.4 \times 10^6$ K for (a) $R_m = 1.4R_\odot$, (b) $R_m = 1.69R_\odot$, and (c) $R_m = 2.4R_\odot$. Vertical arrows denote critical points.

velocity is considerably less, 120 grid points corresponding to a step length $0.013R_\odot$ were needed to prevent the onset of spurious downdrafts at the base.

6. Results and Discussion

The computations were carried out for both isothermal and polytropic cases, the latter in greater detail as it permits a realistic variation of temperature to be considered. Let us first examine the results of the isothermal case. We selected a form for $A(r, t)$ given by Equation (3.1) assuming a choice $\theta_i \sim 4°$, which corresponds to a base area $\sim 2 \times 10^9$ km^2, and $\Delta\theta \sim 3°$, which implies an area at R_m about 3 times larger than would exist if the tube were radial. Figures 2 and 3 depict the spatial variation of velocity and density at certain instants of time for different values of R_m, assuming a time constant $\tau = 1000$ s and an isothermal temperature $T = 3.4 \times 10^6$ K (this corresponds to a sound speed ~ 240 km s^{-1}). In each of these figures, the dotted and dashed curves denote the initial and final steady states respectively (as calculated from Equations (2.1)–(2.3) without the $\partial/\partial t$ terms). The initial state common to all the figures, depicts the isothermal solar wind solution with a single critical point located at $1.69R_\odot$. Certain features can be discerned in the time-dependent solutions. Firstly, we observe that starting from a common initial solution, different final steady solutions that depend upon R_m are possible. The time-dependent solutions appear asymptotically to approach these steady solutions. Secondly, as R_m increases, the time-scale for the achievement of a steady state decreases. In Figures 2a and 3a, where $R_m = 1.4R_\odot$, the solution at $t = 15\,000$ s is still quite distinct from the steady solution. As R_m increases, we see that the solution approaches the steady state within a shorter time. In Figures 2c and 3c for $R_m = 2.4R_\odot$, the solution at $t = 11\,800$ s practically merges with the steady state. This behaviour is related to the fact that a sudden change occurs in the steady state topology when R_m approaches the critical point at $1.69R_\odot$. The sonic point moves inwards and a transition to a state which supports a faster flow takes place. This transition occurs because a small decrease in R_m close to $1.69R_\odot$ results in a sudden change in topology from one with a single critical point to another with three such points. The sonic transition here is at the innermost critical point. Similar behaviour was also noted by Steinolfson and Tandberg-Hanssen (1977) for steady flow. When studying time-dependent problems, this feature reveals itself through the fact that the gradients of the flow variables are more pronounced in the transients than in the final steady state. Thus, we expect the time-scale for the attainment of a steady state to increase with decreasing R_m.

Lastly, we find that when more than one critical point exists, the transients still appear to approach the final physical solution. We can see this in Figure 2a for $R_m = 1.4R_\odot$, where the final state has three critical points (indicated by vertical arrows), one of course at $1.69R_\odot$ since the flow is radial beyond $1.4R_\odot$ and two more between $1R_\odot$ and $1.4R_\odot$. The sonic transition in the steady solution occurs at the innermost critical point.

We now consider the results for the polytropic case. Here the second form for the area given by Equation (3.2) was used. Following KH, we choose $R_1 = 1.5R_\odot$ and $\sigma = 0.1R_\odot$. Figures 4 and 5 show the spatial variation of the flow variables at different

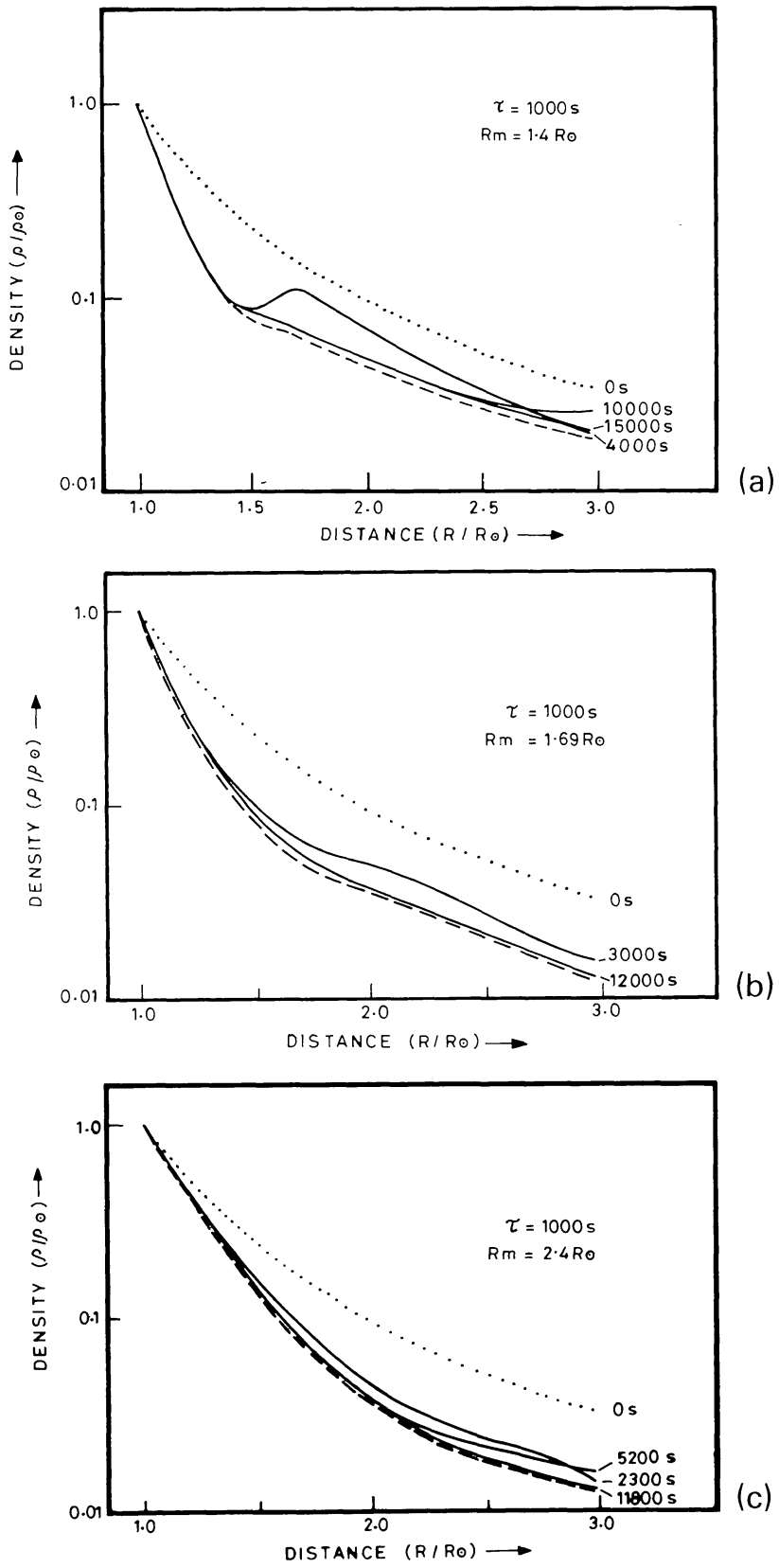

Fig. 3. The radial variation of density at different instants of time is shown in the isothermal case assuming $\tau = 1000$ s and $T = 3.4 \times 10^6$ K for (a) $R_m = 1.4R_\odot$, (b) $R_m = 1.69R_\odot$, and (c) $R_m = 2.4R_\odot$.

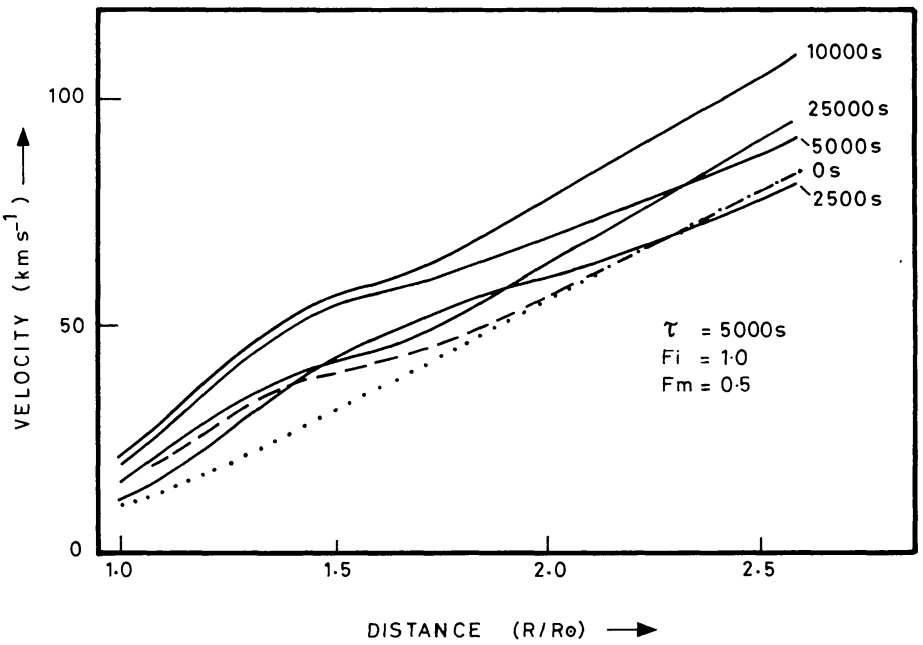

Fig. 4a.

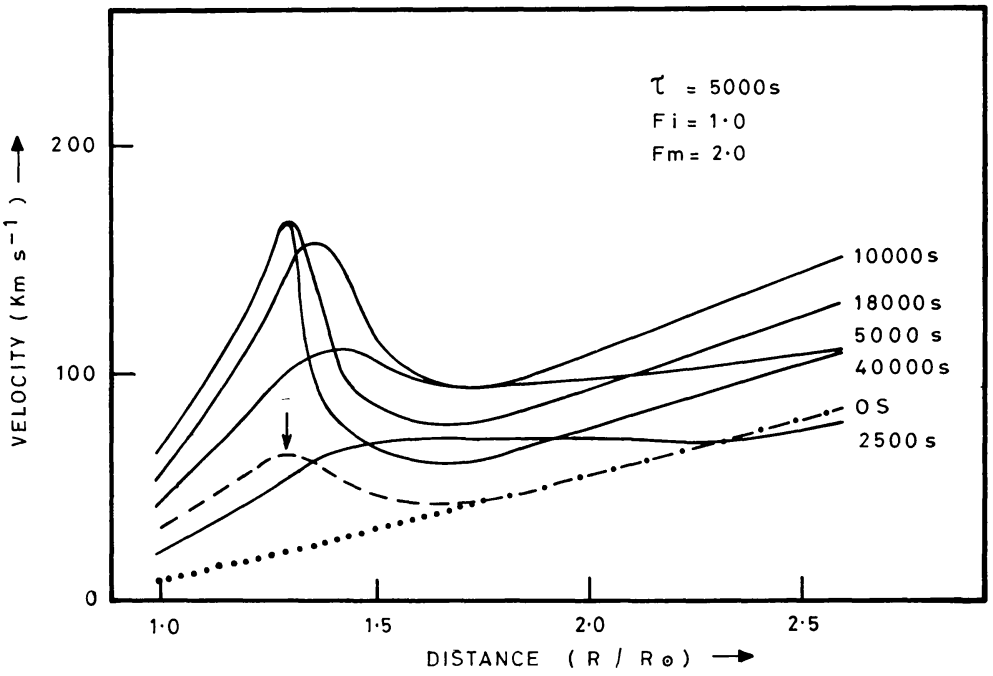

Fig. 4b.

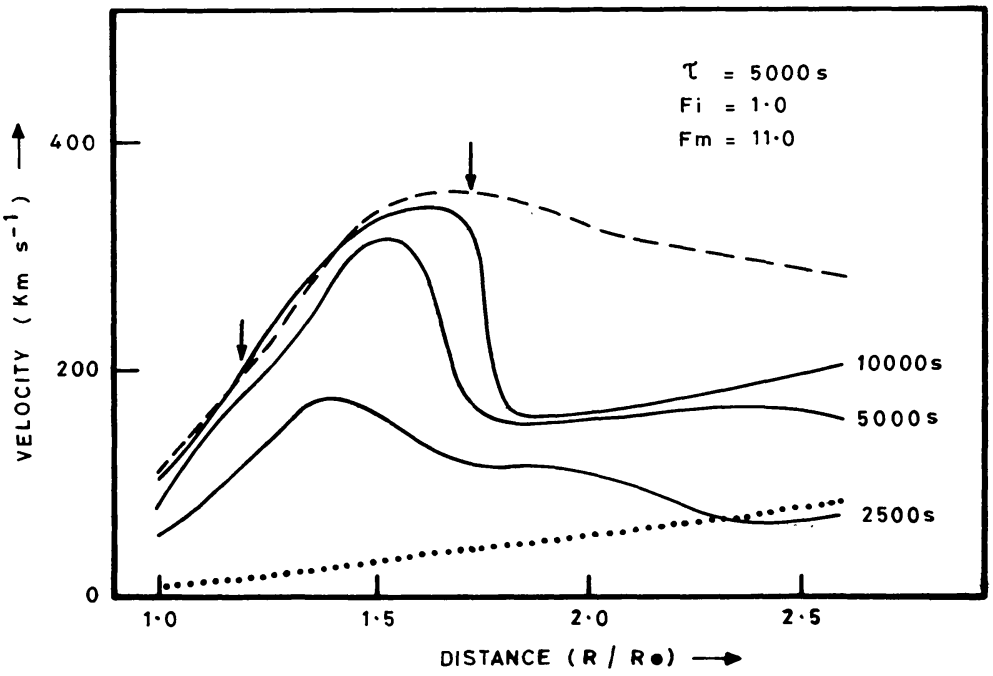

Fig. 4c.

Fig. 4a–c. Velocity as a function of radial distance is shown at different instants of time in the polytropic case assuming $\tau = 5000$ s, $E = 1.8 \times 10^{15}$ erg g^{-1} and $F_i = 1.0$ for (a) $F_m = 0.5$, (b) $F_m = 2.0$, and (c) $F_m = 11.0$. Vertical arrows denote critical points.

times for various values of F_m, assuming $F_i = 1$ (i.e. an initial radial variation of tube geometry), a time constant $\tau = 5000$ s and $E = 1.8 \times 10^{15}$ erg g^{-1} (this leads to a base temperature of 2×10^6 K). Consider first Figures 4a and 5a for which $F_m = 0.5$ (i.e. $f_{\max}(\infty) = 1.5$). The dotted curve depicts the usual polytropic solar wind solution, which for $\alpha = 1.1$ has a sonic transition at $4.5R_\odot$. The final steady state which has a single critical point is also shown in Figure 4a. We observe that the transient solutions overshoot the steady solution, but after around 10000 s gradually begin to 'relax' towards it. Figures 4b and 5b show the situation for $F_m = 2$. The final steady state for this value of F_m has three critical points, with a sonic transition at the outermost critical point. The transient solutions in this case show a considerable departure from the steady state that we have just mentioned. At $t \sim 18000$ s a spatial discontinuity, whose position remains fixed in time can be observed in Figure 4b. We identify this discontinuity as a standing shock. The flow on either side of the shock approaches different branches of the steady state topology. We may also note that for such a discontinuous asymptotic state, the sonic transition occurs three times, once at the inner critical point, the second time at the shock and lastly at the outer critical point at $4.5R_\odot$. Figures 4c and 5c show the flow pattern for $F_m = 11$. Again a shock-like discontinuity is observed to develop, in this case around $t \sim 8000$ s. The solution on the two sides of the shock is again seen to approach different branches of the corresponding steady state topology. It may be noted, however, that there is only one sonic transition, which occurs at the innermost critical point.

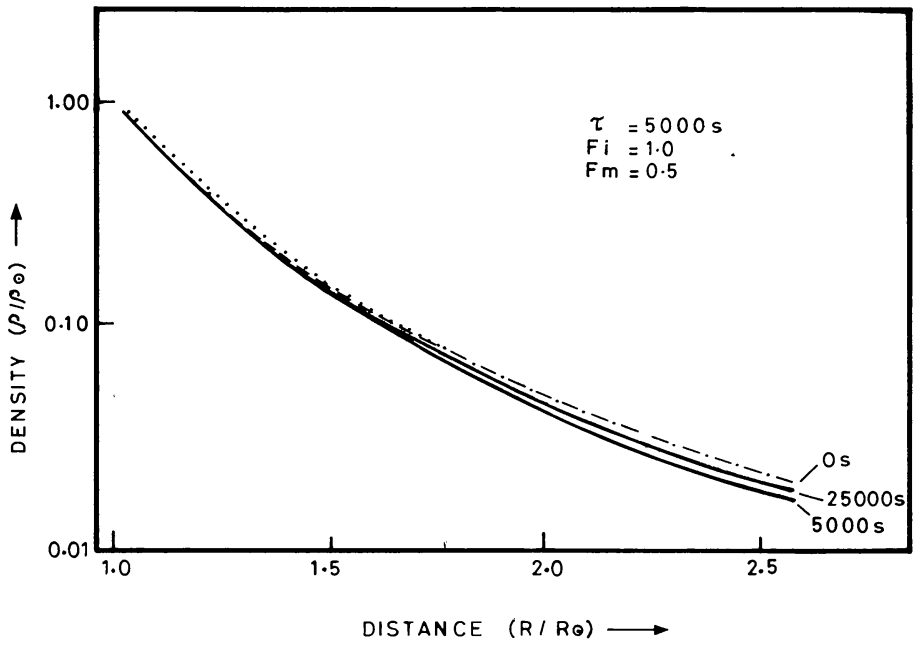

Fig. 5a.

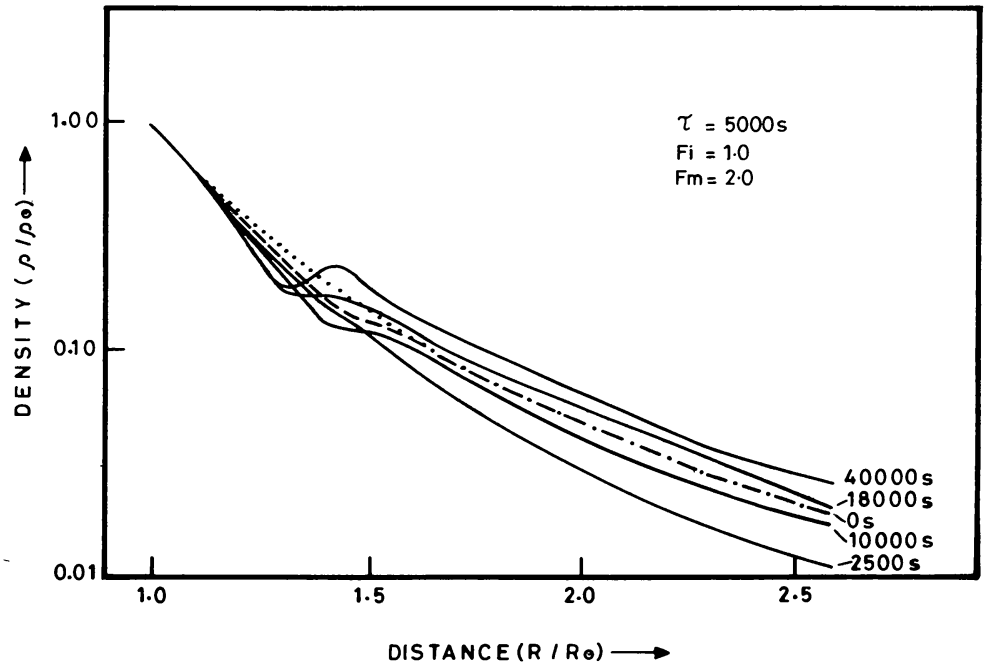

Fig. 5b.

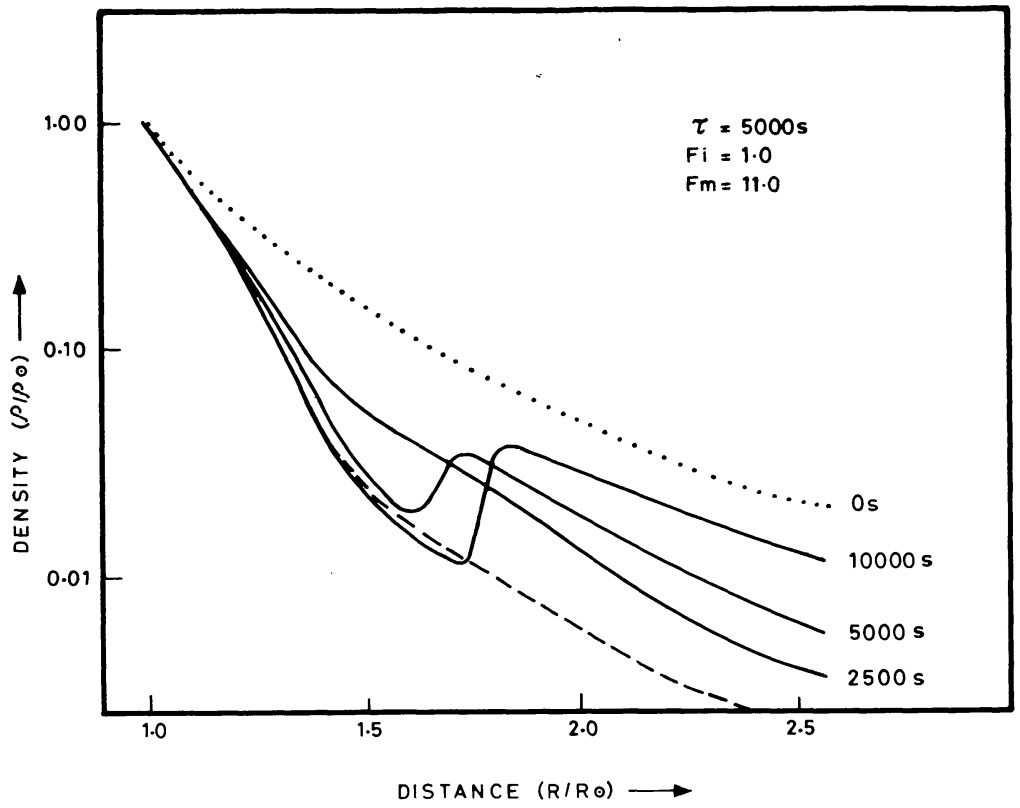

Fig. 5c.

Fig. 5a–c. Density as a function of radial distance is shown at different instants of time in the polytropic case assuming $\tau = 5000$ s, $E = 1.8 \times 10^{15}$ erg g^{-1} and $F_i = 1.0$ for (a) $F_m = 0.5$, (b) $F_m = 2.0$, and (c) $F_m = 11.0$.

Consider now the situation when the change in geometry occurs on a slower time-scale. Figures 6a and 6b depict the velocity and density distribution for $\tau = 15\,000$ s, assuming $F_m = 2$. The velocity gradients that appear in the transient solutions are less pronounced than for $\tau = 5000$ s (compare with Figure 4b). Asymptotically, the transients appear to approach the smooth steady state. We thus see that the final stationary state can depend upon the rapidity with which the geometry changes. In order to appreciate this behaviour, it is instructive to note that whereas changes in flow geometry occur on a time-scale τ, the time-scale for the flow variables to respond to these changes is different. This response time of the system depends upon the swiftness with which changes in geometry are communicated to the flow variables by the C_+, C_0, and C_- characteristics. If τ is sufficiently small, then large transient effects can occur, permitting for certain cases steep enough gradients to develop in the flow variables so that a discontinuity in the form of a shock appears. Physically, a shock makes it possible to link two unconnected branches in the steady flow topology.

Lastly, consider Figures 7a and 7b which depict the solutions for a nonradial initial state ($F_i = 7.4$), an asymptotic state characterized by $f_{\max}(\infty) = 8$ and $\tau = 15\,000$ s. The motivation for studying this case arose from the result obtained for steady flow by KH that as $f_{\max}$ increases, a dramatic transition occurs in the solution topology at

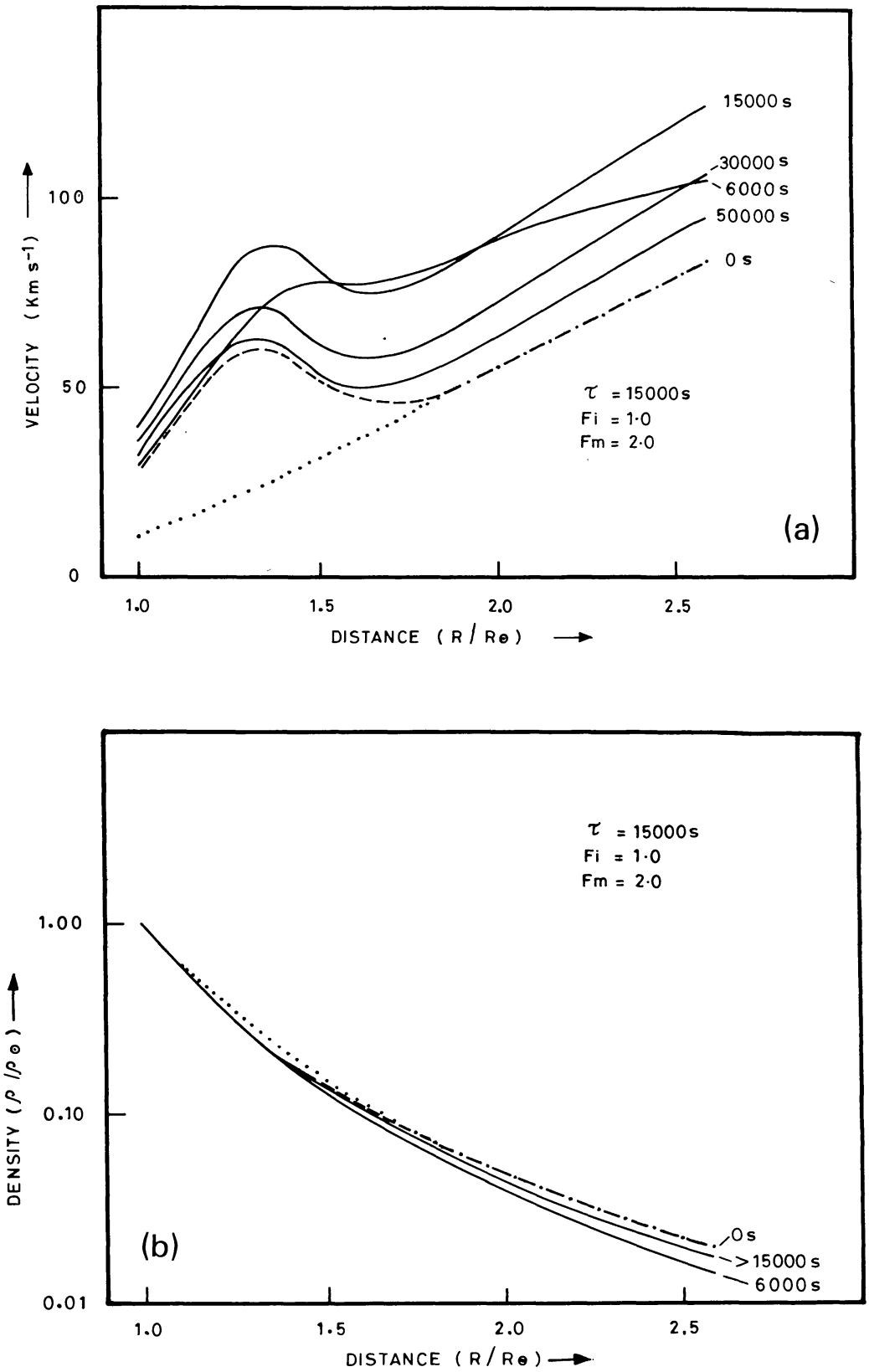

Fig. 6. Radial profiles of (a) velocity and (b) density at different times are plotted for a polytropic flow assuming $\tau = 15000$ s, $E = 1.8 \times 10^{15}$ erg g^{-1}, $F_i = 1.0$ and $F_m = 2.0$.

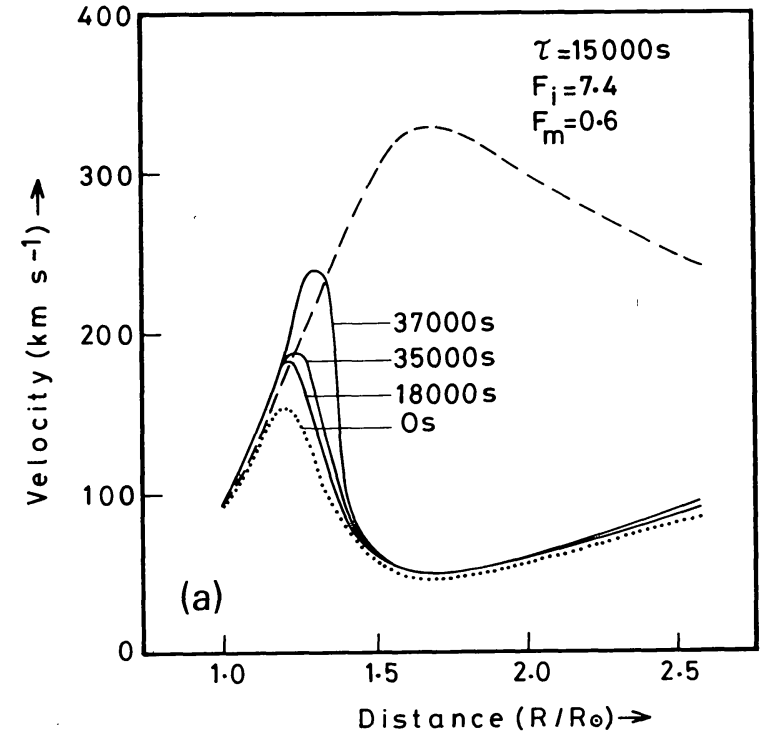

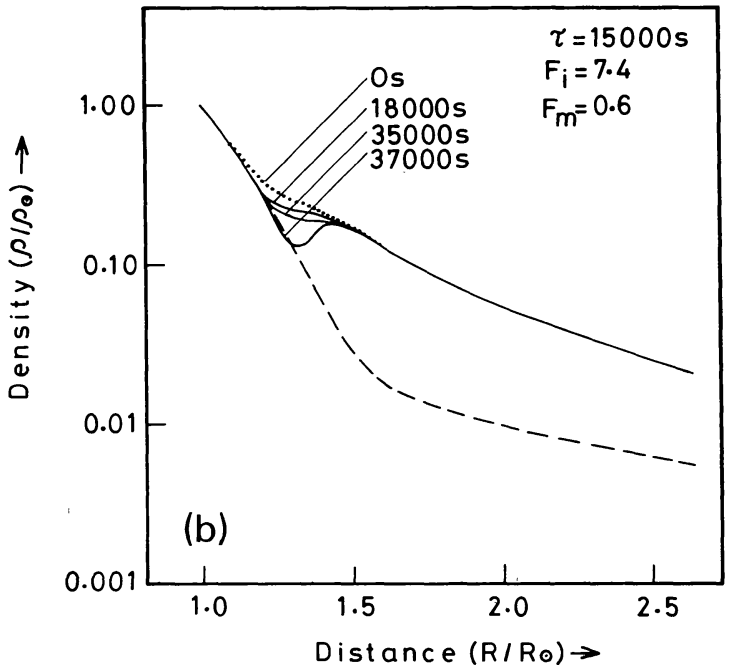

Fig. 7. Radial profiles of (a) velocity and (b) density at different times are plotted for a polytropic flow assuming $\tau = 15000$ s, $E = 1.8 \times 10^{15}$ erg g^{-1}, $F_i = 7.4$ and $F_m = 0.6$.

$f_{max} \sim 7.5$. An increase of f_{max} beyond 7.5 leads to a shift of the sonic transition from the outermost critical point to the innermost critical point. From the analysis of KH, it is not clear how the transient adjustment between the two states proceeds as the value 7.5 for f_{max} is crossed. This can, however, be discerned from the results of our time-dependent study. In Figure 7a, we find that between 18 000 s and 35 000 s the velocity profiles change comparatively little. However, note that between 35 000 s and 37 000 s there is a dramatic increase in the velocity, especially around $1.4R_\odot$, suggesting the occurrence of a sudden change in the character of the solution. There is also a corresponding dip in the density, though the effect is not so pronounced. We identify this sudden change in the flow profiles as being related to the transition predicted by steady state analysis at $f_{max} \sim 7.5$. It is worthwhile mentioning that the transitions in the time-dependent solution does not occur at the value of t for which $f_{max}(t) \sim 7.5$ but later in view of the finite response time of the system. It would have been interesting to follow the temporal development of the flow beyond $t = 37\,000$ s, but this would have been prohibitive in terms of computer time.

The results obtained in the previous sections highlight several interesting points. Starting from an initial steady critical solution in a radial geometry, a transition to a smooth and continuous final steady state in a geometry diverging faster than r^2 is possible even in the presence of multiple critical points, provided the change in geometry does not proceed too swiftly. When multiple critical points arise, the final steady state can become supersonic at any one of these points. In practice for steady flow, one usually has to select the relevant solutions from physical considerations. On the basis of our time-dependent study, we find that when the change in geometry is gradual enough, the asymptotic state automatically 'selects' the steady branch that is single-valued and extends continuously outwards from the Sun. However, for sufficiently rapid changes in geometry, in certain cases a standing shock appears and the asymptotic state is completely different from the one just mentioned. The formation of a shock is related to the occurrence of a region where the flow becomes locally compressive. In such a region, the velocity gradient becomes negative and the density gradient positive. For a shock to form, the gradients should become so steep that the flow variables are no longer single-valued. The sharpness of the flow profile at any instant of time depends both upon the spatial as well as temporal gradients of $A(r, t)$. In the isothermal case, a study of the flow for the parameters considered did not lead to shock formation, though the gradients in the transient solutions became more pronounced when R_m (the effective length for nonradial divergence) was decreased (for fixed τ and same degrees of divergence). The polytropic study for different f_{max} (i.e. for different degrees of nonradial divergence) showed that shock solutions are possible in certain cases (e.g. $F_i = 1$ and $F_m = 2, 11$) depending upon the choice for τ. Thus, we see that the occurrence of shocks is related to the detailed form of $A(r, t)$. No straightforward criterion for shock formation appears to emerge on the basis of the present investigation.

7. Application to Coronal Holes

Let us now turn to the application of our study to coronal holes. Since coronal holes exhibit temporal changes, especially during their initial phases (Krieger, 1977), we adopted a time-dependent approach to model the flow within them. We assume that the geometry is radial initially and that the development of a coronal hole is characterized by the geometry becoming nonradial, with the degree of nonradial divergence increasing with time. After a certain time the geometry becomes almost stationary. In our picture, this state corresponds to a fully developed coronal hole, which we assume exists for a sufficient length of time. By considering certain specific forms for $A(r, t)$, which were chosen to mimic the actual geometry of evolving coronal holes, the time-dependent flow in them was studied. An important result that emerges from our study is that starting from a normal solar wind solution, several final states characterized by various degrees of nonradial divergence are possible. For the case, when the geometry evolves sufficiently gradually, one finds that as the degree of nonradial divergence increases the flow speed within the holes is enhanced and the density decreases. However, if the evolution is rapid enough, shock-like solutions are also possible. The number of such solutions (depending upon how rapidly the geometry changes) may be arbitrarily large corresponding to the number of ways one can devise to connect unrelated branches in the steady state topology. Thus, there exists the possibility of having localised enhanced flows even in geometries with a low amount of nonradial divergence.

In our study of the polytropic time-dependent flow, we chose an initial state which corresponds to a high speed solar wind at 1 AU. This is implicit in the value of E, the energy per gram, we adopted when examining the polytropic solutions. Our choice of $E = 1.8 \times 10^{15}$ erg g^{-1} leads to a flow velocity of 600 km s^{-1} at infinity. The answer to the question of how such a high speed stream is produced to begin with has not been attempted by us. At present the detailed nature of the processes which are responsible for the high wind speeds observed at 1 AU is not satisfactorily understood (Holzer, 1979). We have implicitly assumed that by some unspecified mechanism, an initial state corresponding to a high speed wind (at 1 AU) is first established and changes in geometry that characterize the development of a coronal hole after its birth occur subsequently. Even if this mechanism were to operate simultaneously with changes in geometry, the essential nature of our results is unlikely to be altered. This question will, however, be analysed quantitatively in a forthcoming paper.

Finally, let us discuss some observational implications of our study. We have shown that the final state obtained as a result of changes in geometry can depend on the rapidity of this change. The actual values used for τ were only for illustrative purposes. In order to relate these two observations, one should look at the temporal evolution of coronal holes (CH for short) immediately after their formation. Although observations show that the areas of CH regions grow and decay at a mean rate of 10^9 km^2 day^{-1} (Bohlin, 1977), which is consistent with the diffusion rate of magnetic fields obtained by Leighton (1964), there is some doubt about the actual time of formation of CH regions. The sole observations of Solodyna *et al.* (1977) about the birth of a CH show a time-scale nearly

one third of the diffusion timescale, and even this may be only an upper limit, since observations separated by less than 9 hr were not available.

It is perhaps possible that the actual evolution of a CH region is characterized by two time-scales. The first is the diffusion time-scale which decides the areal extent over which reconnection or the MHD process responsible for changes in field topology has spread. This ties in well with the long term evolution of coronal holes. On the other hand, once a certain area has been 'affected' by the MHD process, changes in geometry might develop on a much faster time-scale. Our work anticipates such a possibility and predicts that shock-like discontinuities may occur when the change in geometry is sufficiently rapid. There are indications that the actual evolution of a CH region is characterized by discrete large scale changes in the CH boundary occurring within time-scales less than a supergranule lifetime (Nolte *et al.*, 1978). It is tempting to speculate that the association of X-ray coronal transients with the boundaries of evolving coronal holes (Webb *et al.*, 1978) may in fact be evidence for rapid changes in coronal hole geometry.

8. Summary

In this paper we have studied the flow of gas in a flux tube whose degree of divergence increased as a function of time. Starting from an initial solar wind flow, the time-dependent fluid equations were solved to analyse the transient response of the flow to changes in tube geometry. The asymptotic solutions, were examined in the time limit when the final stationary geometric configuration had been established. It was observed that the character of the flow could depend upon τ, the time-constant for change in geometry. For sufficiently large τ, we found that the asymptotic solutions were practically identical with the 'physical' solutions (i.e. those obeying the correct boundary conditions and possessing a smooth sonic transition) obtained from the steady state equations. An additional feature that emerges during the investigation was that even when the final steady state had multiple critical points, the sonic transition in the asymptotic state 'automatically' occurred at the same critical point as in the 'physical' solution. However, in the opposite limit of small τ, we found that the asymptotic solutions could possess shock-like discontinuities. Although the existence of such solutions has been known for some time (e.g. Holzer, 1977), they were never seriously considered in past studies of the solar wind, as there appeared no reason a priori why they should be preferred to the 'physical' solutions. We have demonstrated that such solutions are possible in certain cases when changes in geometry occur sufficiently fast.

By choosing suitable forms for the area of a flow tube, it was pointed out that our study provided a framework for studying the flow in evolving CH regions.

Acknowledgements

We appreciate helpful comments by the referee. The computations were carried out on the DEC 1090 system at the Indian Institute of Science, Bangalore.

References

Altschuler, M. D., Trotter, D. E., and Orall, F. Q.: 1972, *Solar Phys.* **26**, 354.

Bohlin, J. D.: 1977, *Solar Phys.* **51**, 377.

Courant, R. and Friedrichs, K. O.: 1948, *Supersonic Flow and Shock Waves*, Interscience, Chapter II.

Hasan, S. S. and Venkatakrishnan, P.: 1980, *Kodaikanal Obs. Bull. Ser. A* **3**, 6.

Hasan, S. S. and Venkatakrishnan, P.: 1981, *Solar Phys.* **73**, 45.

Holzer, T. E.: 1976, in D. J. Williams (ed.), *Physics of Solar Planetary Environments*, AGU, p. 366.

Holzer, T. E.: 1977, *J. Geophys. Res.* **82**, 23.

Holzer, T. E.: 1979, in E. N. Parker, C. F. Kennel, and L. J. Lanzerotti (eds.), *Solar System Plasma Physics*, Vol. I, North-Holland, p. 103.

Hundhausen, A. J.: 1972, *Coronal Expansion and Solar Wind*, Springer-Verlag, New York, Chapter III.

Kopp, R. A. and Holzer, T. E.: 1976, *Solar Phys.* **49**, 43.

Kopp, R. A. and Pneuman, G.: 1976, *Solar Phys.* **50**, 85.

Krieger, A. S.: 1977, in J. B. Zirker (ed.), *Coronal Holes and High Speed Wind Streams*, Colorado Ass. Univ. Press, p. 71.

Krieger, A. S., Timothy, A. F., and Roelof, E. C.: 1973, *Solar Phys.* **29**, 505.

Leighton, R.: 1964, *Astrophys. J.* **140**, 1547.

Munro, R. H. and Jackson, B.: 1977, *Astrophys. J.* **213**, 874.

Munro, R. H. and Withbroe, G. L.: 1972, *Astrophys. J.* **176**, 511.

Nolte, J. T., Gerassimenko, M., Krieger, A. S., and Solodyna, C. V.: 1978, *Solar Phys.* **56**, 153.

Parker, E. N.: 1958, *Astrophys. J.* **128**, 664.

Parker, E. N.: 1960, *Astrophys. J.* **132**, 175.

Parker, E. N.: 1963, *Interplanetary Dynamical Processes*, Interscience, New York–London.

Parker, E. N.: 1965, *Space Sci. Rev.* **4**, 666.

Solodyna, C. V., Krieger, A. S., and Nolte, J. T.: 1977, *Solar Phys.* **54**, 123.

Steinolfson, R. S. and Tandberg-Hanssen, E.: 1977, *Solar Phys.* **55**, 99.

Suess, S. T.: 1979, *Space Sci. Rev.* **23**, 159.

Webb, D. F., McIntosh, P. S., Nolte, J. T., and Solodyna, C. V.: 1978, *Solar Phys.* **58**, 389.

Zirker, J. B. (ed.): 1977, *Coronal Holes and High Speed Wind Streams*, Colorado Ass. Univ. Press, see collection of papers.